Eur. Phys. J. B **2**, 121–129 (1998)

THE EUROPEAN PHYSICAL JOURNAL B

Influence of magneto-coupling between the longitudinal motion component and transverse Landau orbits of an electron on transmission features in single quantum barriers

X.-H. Wang[a], B.-Y. Gu, and G.-Z. Yang

CCAST (World Laboratory) P.O. Box 8730, Beijing 100080, China
Institute of Physics, Academia Sinica, P.O. Box 603 No. 92, Beijing 100080, China

Received: 26 September 1997 / Revised: 26 November 1997 / Accepted: 15 December 1997

Abstract. In this paper we study the influence of the magneto-coupling effect between the longitudinal motion component and the transverse Landau orbits of an electron on transmission features in single barrier structures. Within the parabolic conduction-band approach, a modified one-dimensional effective–mass Schrödinger equation, including the magneto-coupling effect generated from the position–dependent effective mass of the electron, is strictly derived. Numerical calculations for single barrier structures show that the magneto-coupling effect brings about a series of the important changes for the transmission probability, the above–barrier quasi–bound states, and the tunneling time. Through examining the variation of the above–barrier resonant–transmission spectrum with the barrier width and observing the well–defined Lorentzian line–shape of the above–barrier resonant peaks, we convincingly show that the above–barrier resonant transmission in single barrier structures is delivered by the above–barrier quasibound states in the barrier region, just as the below–barrier resonant tunneling in double barrier structures is mediated by the below–barrier quasi–bound states in the well. Furthermore, we come to the conclusion that the magneto–coupling effect brings about not only the splitting of the above–barrier quasi–bound levels but also the striking reduction of the level–width of the quasi–bound states, correspondingly, the substantial increase of the density of the quasi–bound states. We suggest that magneto–coupling effects may be observed by the measurements of the optical absorption spectrum associated with the above–barrier quasi–bound states in the single barrier structures.

PACS. 73.40.Lq Other semiconductor-to-semiconductor contacts, p-n junctions, and heterojunctions – 73.40.Gk Tunneling – 73.20.Dx Electron states in low-dimensional structures (superlattices, quantum well structures and multilayers)

1 Introduction

As the growth techniques of nanostructures reach a high level of perfection, the one-dimensional (1-D) quantum systems, such as quantum wells, single or double potential barrier structures and so on, have been realized in semiconductor heterostructures. These structures are formed by alternating thin layers of different materials, in which the thickness and material for each layer can be controlled with considerable accuracy. In fact, the motion of an electron in these devices is three dimensional (3-D). However, as long as the longitudinal motion component of the electron in the direction perpendicular to interfaces and the transverse motion component of it in the plane parallel to interfaces are completely decoupled (which is referred to subsequently as the decoupled condition of single-electron motion), the longitudinal motion of the electron can be ascribed to the ideal, 1-D quantum problem. In the devices consisting of semiconductor heterostructures, the quantum characteristics of them are primarily governed by the property of quantum motion of electrons in the direction perpendicular to interfaces. Thus, the actual (3-D) problem in these devices can be reduced to 1-D problem. But, the decoupled condition of single-electron motion is quite crucial. As is well-known, the nonparabolicity of the conduction-band leads to the significant deviation from the decoupled condition of single-electron motion. Ekenberg [1] applied envelope-wave function approach to examine the effects of the nonparabolicity of the conduction-band on bound levels in the quantum wells consisting of GaAs/GaAlAs. Boykin *et al.* [2] employed the tight-binding model to investigate the dependence of the tunneling probability and current of electrons on the transverse wave vector $\mathbf{k}_{xy}$ lying in the plane parallel to interfaces in the double-barrier heterostructures consisting of InAs/AlSb. They ascribed the $\mathbf{k}_{xy}$-dependence to the nonparabolicity of the conduction-band of InAs.

[a] e-mail: wangxh@aphy01.iphy.ac.cn

In contrast, it has long been believed that within the parabolic conduction-band approach the decoupled condition of single-electron motion can be satisfied very well. In other works, the coupling effect between normal and lateral degrees of freedom of an electron is frequently omitted within the parabolic conduction-band approach even though it was included in reference [3–5]. However, the recent studies have demonstrated that the effective-mass difference of the electron in different thin layers is sufficient to bring about the significant dependence of the transmission probability on the transverse wave vector $\mathbf{k}_{xy}$ in multi-barriers [6] and single barrier [7] structures at zero magnetic field. More recently, considerable effort has been devoted to the study of magneto-coupling effect between the longitudinal motion of an electron and the transverse Landau orbits of it in semiconductor heterostructures. The dependence of the bound state levels in quantum wells and the minibands in superlattices on the transverse wave number k_{xy} or Landau quantum number N has been examined at zero or finite magnetic fields [8], and the important influence of the magneto-coupling effect on the transmission probability $T_{\rm p}$ through single quantum barriers has also been shortly reported [9].

As inspired by the experimental observations of negative differential resistance [10] and above-barrier quasibound states [11] in single quantum barriers, single barrier heterostructures have received considerable attention in recent years. The theoretical investigations on single barrier heterostructures have involved in transmission probability [7,12,13] and current-voltage characteristics of electrons [13,14]. In addition, renewed attention was paid to phase time [7,15] of electrons in this systems because recent photon tunneling experiments [16] and the comparison between the theoretical phase time and the simulated tunneling time (which is evaluated with the software Interquanta) for electrons [15] have shown that the phase time is a reasonable approximation of the tunneling time for both photonic and electronic tunneling. Even though a great deal of works on single barrier structures were reported, the physical picture of above-barrier resonant transmission has not been directly argued in literature so far. Does the above-barrier resonant transmission in single barrier structures have the physical picture similar to the resonant tunneling in double barrier structures? It still remains open question.

Even though our previous work [9] has concisely reported the significant dependence of the transmission probability $T_{\rm p}$ through a barrier on the transverse Landau quantum number N when taking the magneto-coupling effect into account within the parabolic conduction-band approach, the further and more detailed features remain to be revealed by examining the influence of the magneto-coupling on the tunneling time, the line-shape of the above-barrier resonant peaks, the above-barrier quasibound states, and the densities of them in single barrier structures. Through investigating these problems, we can get a deep and perfect insight into the physical picture of the resonant transmission and the properties of the above-barrier quasibound states in single quantum barriers when the magneto-coupling effect is included. This paper is organized as follows. In Section 2, based upon parabolic conduction-band approach, a modified 1-D effective-mass Schrödinger equation (M-1DEMSE), including the magneto-coupling effect generated from the difference of the effective mass of the electron inside and outside the barrier, is strictly derived for heterostructures. We will show that the magneto-coupling effect leads to an essential change that the effective barrier height seen by electrons is no longer a constant but rather depending on the Landau quantum number N and the magnetic-field intensity B. According to the M-1DEMSE, the analytical expressions of the transmission probability $T_{\rm p}$ and the tunneling time $T_{\rm t}$ (within the phase time approach) are obtained for single barrier structures. They depend on, not only the longitudinal kinetic energy E_z of the incident electron, but also the Landau quantum number N and the magnetic-field intensity B. In Section 3, we carry out the numerical calculations for single quantum barrier to reveal the striking influence of the magneto-coupling on $T_{\rm p}$ and $T_{\rm t}$ in detail. Furthermore, we will examine the variation of the above-barrier resonant transmission spectrum with the barrier width, and the line-shape of the resonant peaks as well as the density of the above-barrier quasibound states in the single quantum barrier. At the same time, we will argue the physical mechanism of the above-barrier resonant transmission in single quantum barriers. Finally, Section 4 contains a brief summary of the main findings in this study and some remarks.

2 Formulas

For semiconductor heterostructures under the action of a longitudinal magnetic field (perpendicular to interfaces, referred to Z-direction), it has long been believed that within the parabolic conduction-band approximation, both the transverse Landau level of an electron and the longitudinal energy component of it are the conservation quantities. This assumption leads to that longitudinal motion of the electron is governed by the 1-D effective-mass Schrödinger equation as follows:

$$-\frac{\hbar^2}{2}\frac{\mathrm{d}}{\mathrm{d}z}\frac{1}{m(z)}\frac{\mathrm{d}}{\mathrm{d}z}\Phi(z)+U(z)\Phi(z)=E_z\Phi(z), \qquad (1)$$

where $m(z)$ is the position-dependent effective mass of the electron, $U(z)$ the effective potential function, and E_z the longitudinal component of energy of the electron. $m(z)$ and $U(z)$ are, respectively, defined as follows:

$$m(z)=\begin{cases} m_{\rm w} & \text{(in the well material)},\\ m_{\rm b} & \text{(in the barrier material)},\end{cases}$$

and

$$U(z)=\begin{cases} 0 & \text{(in the well material)},\\ U_0 & \text{(in the barrier material)},\end{cases}$$

where $m_{\rm w}$ and $m_{\rm b}$ are respectively the effective mass of the electron in the well and barrier materials; U_0 is the offset of the conduction-band edge between two materials. The total energy E of the electron is defined as $E = E_z + E_N$, here E_N is the N-th Landau level of the electron. Equation (1) implies that the longitudinal motion of the electron and the transverse Landau orbit motion of it are completely independent and separable. However, as will be proved in the following paragraph, the conservation quantities are the total energy E of the electron and the transverse Landau quantum number N of it rather than the longitudinal and transverse components of energy of the electron when considering the difference of the electron effective mass in different segments of the structures. Hence, it is essential to make certain modifications for Equation (1).

We now start with the three-dimensional Hamiltonian of single electron in the semiconductor heterostructures upon the application of a longitudinal magnetic field, $\mathbf{B} = (0, 0, B)$. We choose the symmetric gauge for the vector potential as

$$\mathbf{A} = \frac{1}{2}\mathbf{B} \times \mathbf{r}. \tag{2}$$

In the effective-mass parabolic-band approximation, the Hamiltonian of single electron is read as

$$\hat{\rm H} = \frac{1}{2m(z)}[(\hat{\rm p}_x - \frac{eB}{2}y)^2 + (\hat{\rm p}_y + \frac{eB}{2}x)^2] + \frac{1}{2}\hat{\rm p}_z\frac{1}{m(z)}\hat{\rm p}_z + U(z). \tag{3}$$

We follow the standard procedures to introduce the creation operator $\hat{\rm a}^+$ and annihilation operator $\hat{\rm a}$ of a harmonic oscillator, defined by

$$\begin{cases} \hat{\rm a}^+ = (2\hbar eB)^{-1/2}[(\hat{\rm p}_x - \frac{eB}{2}y) + i(\hat{\rm p}_y + \frac{eB}{2}x)], \\ \hat{\rm a} = (2\hbar eB)^{-1/2}[(\hat{\rm p}_x - \frac{eB}{2}y) - i(\hat{\rm p}_y + \frac{eB}{2}x)]. \end{cases} \tag{4}$$

Therefore, we can obtain the expressions of $\hat{\rm p}_x$ and $\hat{\rm p}_y$ in terms of $\hat{\rm a}^+$ and $\hat{\rm a}$

$$\begin{cases} \hat{\rm p}_x - \frac{eB}{2}y = (\frac{\hbar eB}{2})^{1/2}(\hat{\rm a}^+ + \hat{\rm a}), \\ \hat{\rm p}_y + \frac{eB}{2}x = -i(\frac{\hbar eB}{2})^{1/2}(\hat{\rm a}^+ - \hat{\rm a}). \end{cases} \tag{5}$$

As well-known, $\hat{\rm a}^+$ and $\hat{\rm a}$ obey Boson commutation relations

$$[\hat{\rm a}, \hat{\rm a}^+] = 1 \ ; \ [\hat{\rm a}, \hat{\rm a}] = [\hat{\rm a}^+, \hat{\rm a}^+] = 0. \tag{6}$$

Substituting equation (5) into equation (3) and using Boson commutation relations equation (6), the Hamiltonian of the electron can be rewritten as

$$\hat{\rm H} = (\frac{1}{2} + \hat{\rm N})\hbar\omega(z) + \frac{1}{2}\hat{\rm p}_z\frac{1}{m(z)}\hat{\rm p}_z + U(z), \tag{7}$$

where $\omega(z) = eB/m(z)$ is the position-dependent cyclotron-frequency of the electron; $\hat{\rm N} = \hat{\rm a}^+\hat{\rm a}$ is the occupation number operator of the harmonic oscillator. It has the well-known property

$$\hat{\rm N}\Theta_N(x, y) = N\Theta_N(x, y), \tag{8}$$

$$\Theta_N(x, y) = (L)^{-1/2}\exp\{i[\frac{xy}{2l^2} - \frac{x_0(k_y)y}{l^2}]\}\chi_N[x - x_0(k_y)], \tag{9}$$

$$\chi_N(x) = (2^N N!\sqrt{\pi}l)^{-1/2}\exp(-\frac{x^2}{2l^2})H_N(\frac{x}{l}), \tag{10}$$

where $x_0(k_y) = -l^2k_y$, $l^2 = \hbar/eB$ is the radius of the ground cyclotron orbit. $H_N(x)$ is Hermite's polynomial and L^2 is the area of the structure. $\Theta_N(x, y)$ is the harmonic oscillator eigenfunction with Landau index $N = 0,\ 1,\ 2,\ \cdots$.

Equation (7) shows that operator $\hat{\rm N}$ commutes with $\hat{\rm H}$. Hence, the Landau quantum number N is a conservation quantity. It turns out that the Landau level $E_N = (1/2+N)\hbar\omega(z)$ should be position-dependent when considering the difference of the electron effective-mass in two different materials. Therefore, the Landau level of the electron in the whole structure does not keep conservation. As a consequence, the longitudinal energy $E_z = E - E_N$ of the electron also is no longer the conservation quantity because the total energy of the electron is conserved.

In terms of equation (8), the 3-D wave function of the electron for Hamiltonian $\hat{\rm H}$ of equation (7) can be written a form of variable separation as

$$\Psi(\mathbf{r}) = \Theta_N(x, y)\Phi(z). \tag{11}$$

Substituting this form of wave function into the eigen equation

$$\hat{\rm H}\Psi(\mathbf{r}) = E\Psi(\mathbf{r}), \tag{12}$$

we then find that the longitudinal envelope wave function $\Phi(z)$ is determined by a modified 1-D effective-mass Schrödinger equation (M-1DEMSE), including the magneto-coupling effect, as follows:

$$-\frac{\hbar^2}{2}\frac{\rm d}{{\rm d}z}\frac{1}{m(z)}\frac{\rm d}{{\rm d}z}\Phi(z) + U_{\rm c}(z)\Phi(z) = E_z^{\rm w}\Phi(z), \tag{13}$$

where $E_z^{\rm w}$ is the longitudinal energy of the electron in the well material and $U_{\rm c}(z)$ the effective coupling potential function. They are given by

$$E_z^{\rm w} = E - (\frac{1}{2} + N)\hbar\omega_{\rm w}, \tag{14}$$

and

$$U_{\rm c}(z) = \begin{cases} 0 & \text{(in the well material)}, \\ U(N, B) & \text{(in the barrier material)}, \end{cases} \tag{15}$$

where $U(N,B)$ is the effective barrier height seen by the electron in the barrier material and given by

$$U(N,B) = U_0 - (1-\gamma)(\frac{1}{2}+N)\hbar\omega_{\rm w}, \tag{16}$$

where $\gamma = m_{\rm w}/m_{\rm b}$, and $\omega_{\rm w} = eB/m_{\rm w}$ is the cyclotron-frequency of the electron in the well material.

Comparing equation (1) with equation (13), we can find that there exist two fundamental distinctions between them. The first one is that E_z in equation (1) is now replaced by $E_z^{\rm w}$ in equation (13). From the physical viewpoint, E_z in equation (1) represents the longitudinal energy belonging to the whole structure, irrespective of discontinuity of the electron effective-mass in different materials. It implies that both the longitudinal and transverse components of energy of the electron are the conservation quantities. However, $E_z^{\rm w}$ in equation (13) only belongs to the well material and its appearance reveals explicitly the fact that the above-mentioned conservation is broken at all. The second one lies on the difference of the effective barrier height seen by the electron in the two equations. The effective barrier height in equation (1) is a constant U_0 only determined by the offset of the conduction-band edge in two materials, but it is a varying quantity $U(N,B)$ in equation (13), depending on both the Landau quantum number N and the magnetic-field intensity B. The introduction of the magneto-coupling term $-(1-\gamma)(N+\frac{1}{2})\hbar\omega_{\rm w}$ in $U(N,B)$ is a mathematical price that we have to pay while the variable separation method is used for solving the Schrödinger equation to treat a 3D-problem with use of a 1D equation. This clearly reflects the existence of the magneto-coupling effect between the longitudinal motion component of the electron and the transverse Landau orbits of it.

To recognize the importance of the magneto-coupling effect, we now apply equation (13) to investigate its influence on magnetic transmission of the electron in single quantum barriers. According to equation (13), the longitudinal envelope-wave function can be expressed as

$$\Phi(z) = \begin{cases} \exp(ik_{\rm w}z) + R\exp(-ik_{\rm w}z) \\ \qquad\qquad \text{(in the incident region)}, \\ A_1\exp(-k_{\rm b}z) + A_2\exp(k_{\rm b}z) \\ \qquad\qquad \text{(in the barrier region)}, \\ S\exp(ik_{\rm w}z) \\ \qquad\qquad \text{(in the transmitted region)}, \end{cases} \tag{17}$$

where $k_{\rm w} = (2m_{\rm w}E_z)^{1/2}/\hbar$; $k_{\rm b} = \{2m_{\rm b}[U(N,B) - E_z]\}^{1/2}/\hbar$ and $k_{\rm b}$ is an imaginary when $E_z > U(N,B)$; and here E_z represents the longitudinal energy of an incident electron. If the complex transmission coefficient S is expressed in the form of $S = \mid S \mid {\rm e}^{i\theta}$, the transmission probability $T_{\rm p}$ and tunneling time $T_{\rm t}$ (see Ref. [11]) can be evaluated in terms of $|S|$ and θ by the relations:

$$\begin{cases} T_{\rm p} = \mid S \mid^2, \\ T_{\rm t} = (m_{\rm w}/\hbar k_{\rm w})(\partial\theta/\partial k_{\rm w} + b), \end{cases} \tag{18}$$

here b is the barrier width. By using the continuity conditions for both $\Phi(z)$ and its derivative $\Phi'(z)/m(z)$ at each interface, we can derive the analytical expressions of $T_{\rm p}$ and $T_{\rm t}$ as follows:

$$T_{\rm p} = \frac{4}{[(\gamma\beta)^{-1} + \gamma\beta]^2\sinh^2(k_{\rm b}b) + 4} \tag{19}$$

and

$$T_{\rm t} = \frac{m_{\rm w}\{k_{\rm b}^{-1}[1+\gamma^{-1}+\gamma\beta^2+(\gamma\beta)^{-2}]\}}{\hbar k_{\rm w}\{[(\gamma\beta)^{-1}+\gamma\beta]^2\}} \times \frac{\{\sinh(2k_{\rm b}b) - 2[(\gamma\beta)^{-2}-1]b\}}{\{\sinh^2(k_{\rm b}b)+4\}}, \tag{20}$$

where $\beta = k_{\rm b}/k_{\rm w}$.

3 Numerical results and analyses

We now employ equations (19) and (20) to numerically evaluate the values of $T_{\rm p}$ and $T_{\rm t}$ for single quantum barriers consisting of GaAs/$Ga_{1-x}Al_xAs$ with $x = 0.4$, yielding the offset of the conduction-band edge, $U_0 = 0.296$ eV. In this structure, the effective-masses of the electron in GaAs and $Ga_{0.6}Al_{0.4}As$ are, respectively, $m_{\rm w} = 0.067m_0$ and $m_{\rm b} = 0.101m_0$, here $m_0 = 9.1094 \times 10^{-31}$ kg is the free-mass of the electron.

3.1 Transmission probability

The dependence of the transmission probability $T_{\rm p}$ on the longitudinal energy E_z of the incident electron for several magnetic-field intensities B and Landau quantum numbers N is shown in Figures 1a and 1b for the single barrier structures with the barrier width of 60 Å. Three sets of curves correspond to different magnetic-field intensities of $B = 5, 10$, and 15 tesla, respectively. The consecutive sets of curves have been vertically shifted for clarity. In Figures 1a and 1b, all the curves labeled by the legent a (see the legends in Figs. 1a and 1b) correspond to the case of neglecting the magneto-coupling effect, and other curves associated with the legends b, c, and d to the cases of including the magneto-coupling effect, with different Landau quantum numbers of $N = 0$, 2, and 4, respectively. From Figure 1a, it is clearly seen that the transmission probability of the incident electron in the low energy region increases rapidly as increasing the magnetic field intensity B and Landau quantum number N. For example, when $E_z = 20$ meV, comparing with the value of $T_{\rm p}$ without the magneto-coupling, the relative changes in $T_{\rm p}$ for $N = 0$, 2, and 4 reach, respectively, up to 113%, 142%, and 176% at $B = 5$ T; 120%, 185%, and 272% at $B = 10$ T; as well as 127%, 237%, and 408% at $B = 15$ T. From Figure 1b, it can be seen that in the high energy region of $E_z \geq 0.2$ eV, only one much broad transmission resonant bump above barrier can be resolved when the magneto-coupling effect is neglected; while considering the magneto-coupling effect, it makes not only the first

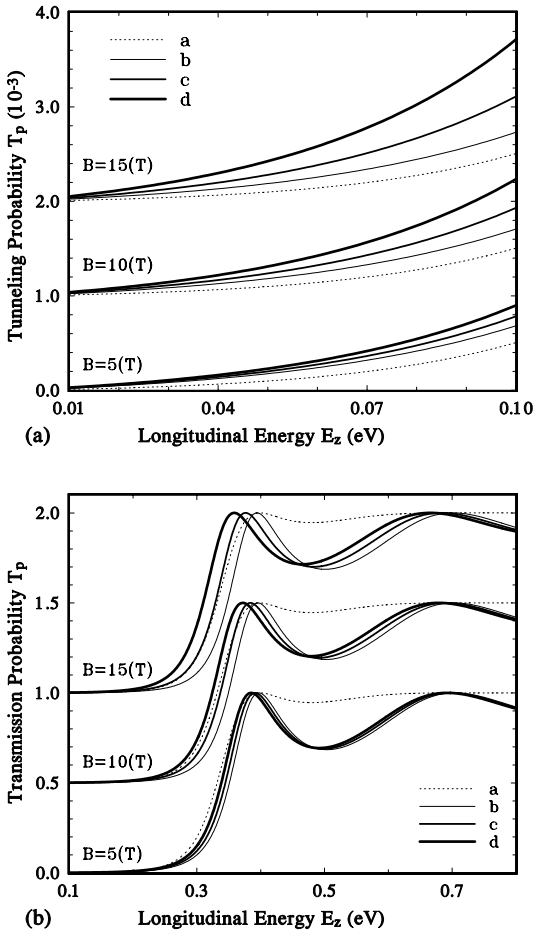

Fig. 1. Influence of the magneto-coupling on the transmission probability T_p as a function of longitudinal energy E_z in single quantum barrier with barrier width of 60 Å for three different magnetic-field intensities, marked in the figure. Two consecutive sets of curves have been vertically shifted for clarity. Curves labeled by a correspond to the case of neglecting the magneto-coupling effect and curves labeled by b, c, and d to the case of including this effect with different Landau quantum indexes of $N = 0$, 2, and 4, respectively. (a) $T_\mathrm{p} - E_z$ curves in the low energy region; (b) $T_\mathrm{p} - E_z$ curves in the high energy region.

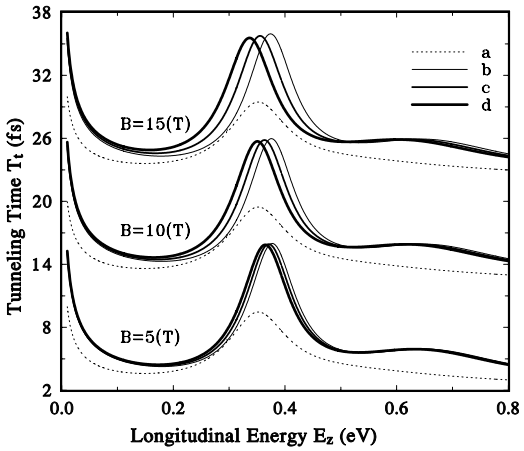

Fig. 2. Influence of the magneto-coupling on the tunneling time spectrum, $T_\mathrm{t} - E_z$, in the same single barrier structure as Figure 1 under three different magnetic fields, as marked in figure. The consecutive sets of curves have been vertically offset for clarity. The legends a, b, c, and d have the same explanation as Figure 1.

peak narrower but also the second broader peak resolvable. At the same time, the magneto-coupling effect leads to a shift of the energy positions of the above-barrier resonance peaks toward the low energy region. Moreover, as increasing the magnetic-field intensity B and the Landau quantum number N, the amounts of the shift increases. For $N = 0$, 2, and 4, the amounts of the shift for the first resonant peak are, respectively, 1, 7, and 13 meV at $B = 5$ T; 3, 14, and 26 meV at $B = 10$ T; 5, 22 and 40 meV at $B = 15$ T. The shift of the resonant peak positions can be easily understood. From the condition of the transmission resonance, $k_\mathrm{b}b = m\pi$, we find the resonant levels as

$$E_{\mathrm{m},N} = E_\mathrm{m} - (1-\gamma)(N+\frac{1}{2})\hbar\omega_\mathrm{w}, \tag{21}$$

where the E_m represents the resonant levels when neglecting the magneto-coupling effect, given by

$$E_\mathrm{m} = \frac{\hbar^2}{2m_\mathrm{b}}\frac{m^2\pi^2}{b^2} + U_0 \qquad (m = 1, 2, 3, \cdots). \tag{22}$$

Equations (21) and (22) clearly show that for a given m, the magneto-coupling effect leads to the fall of the resonant levels as increasing B and N. Therefore, the resonant peaks shift toward the low energy region. In addition, we also see that the magneto-coupling effect brings about the striking reduction of the line-width of the resonant peaks. All the above-mentioned results have evidently demonstrated that the influence of the magneto-coupling effect on the transmission probability is quite pronounced.

3.2 Tunneling time

We now are in a position to investigate the influence of the magneto-coupling effect on the tunneling time T_t. The dependence of T_t on the longitudinal energy E_z of the incident electron for several magnetic-field intensities B and different Landau quantum numbers N is displayed in Figure 2 for the same structure as in Figure 1. The meaning of the legend symbols a, b, c, and d in Figure 2 is the same as in Figure 1. Three sets of curves correspond to different B's of 5, 10, and 15 T, respectively. For clarity, the consecutive sets of curves have been vertically offset. From Figure 2 we can see that the magneto-coupling effect leads to

the increase of the tunneling time T_t. Moreover, there exists an interesting resonance-like phenomenon in the tunneling time spectrum similar to resonance phenomenon appearing in the transmission probability. The magneto-coupling effect results in the shift of the peak positions in T_t which explicitly depends on the magnetic field intensity B and the Landau quantum number N similar to the dependence of the resonant peak positions in T_p on B and N. Furthermore, the positions of resonance-like peaks in T_t are quite close to those of the corresponding resonance peaks in T_p for the given N and B. At the same time, we can see that the increase of the tunneling time T_t caused by the magneto-coupling effect is the most remarkable in the vicinity of the peak positions. Comparing with the peak values without the magneto-coupling effect, the relative increase of the peak height reaches, approximately, up to 60%.

To get a better understanding of these results, it is necessary to do further discussions on the physical mechanism of the resonant transmission in single barrier structures. As well-known, the resonant tunneling in double-barrier structures is mediated by the quasibound states in the well which arise from the multiple coherent reflections of the electronic wave function at the boundaries of the double-barrier scattering potential. Similarly, we may reasonably regard the resonant transmission in single quantum barrier as being generated from multiple coherent reflections of the electronic wave function at two edges of the barrier, leading to the above-barrier quasibound states in the barrier region. Consequently, the incident electron with the longitudinal energy in the vicinity of the above-barrier quasi-bound level is favorable to trap and reside in the barrier region. Thus, it make the corresponding tunneling time T_t longer and then leads to the resonance-like phenomenon in T_t spectrum. The increase of the peak height in T_t spectrum in presence of the magnetic field reflects the fact that the magneto-coupling effect leads to the enhancement of localization of the above-barrier quasibound states. It is also corroborated with the reduction of the the line-width of the resonant peaks in T_p spectrum in presence of the magnetic field, as seen in Figure 1b.

3.3 Variation of transmission probability spectrum with barrier width

To get a further insight into the influence of the magneto-coupling on the above-barrier quasi-bound states, we now examine the variation of the above-barrier resonant-transmission spectrum with the barrier width. $T_p - E_z$ curves above the barrier height are plotted in Figure 3 for three different barrier widths of 90, 120, and 150 Å. Dotted curves correspond to the case of neglecting the magneto-coupling effect and solid curves to the case of including it for $B = 5$ T and $N = 0$. The consecutive sets of curves have been vertically shifted for clarity. From these curves, we can find that the resonant peaks shift toward the low energy region and their line-widths rapidly narrow down as broadening the barrier width. We have pointed out in the last subsection that the above-barrier resonant transmission in single barrier structures has the physical picture similar to the below-barrier resonant tunneling in double barrier structures, *i.e.*, the resonant transmission in single barrier occurs when the longitudinal energy of the incident electron is coincident with one of the above-barrier quasi-bound levels. Thus, the quasi-bound levels are determined by equations (21) and (22), that is to say, the above-barrier quasi-bound levels fall with the increase of the barrier width. So, we can draw a conclusion that the increase of the barrier width leads to the blue-shift of the optical absorption peaks related to these above-barrier quasi-bound levels. On the other hand, the narrowing of line-width of the transmission peaks manifests the reduction of the level width of the quasi-bound states. It leads to the increase of the density of the quasi-bound states (DOQBS). Note that the optical absorption coefficient related to the quasi-bound states is proportional to the DOQBS. Therefore, it can be inferred that the peak intensity of optical absorption spectrum in single quantum barriers enhances as broadening the barrier width. The above two conclusions on the optical absorption spectrum have been confirmed by the experimental results of Luo *et al.* [11] in the single quantum barriers made of the magnetic material ZnMnSe. In their experiment, they chose single quantum barrier structure made of magnetic material in order to utilize the well-known Zeeman effect to produce splitting of the absorption peaks for revealing the existence of the magneto-quasi-bound states in single quantum barriers. We now ask the question: Is it possible to detect the above-barrier magneto-quasi-bound states in single barriers made of non-magnetic materials upon the application of magnetic field? The answer is positive when considering the magneto-coupling effect in the structures. Let us discuss this problem in detail. As indicated above, the magneto-coupling effect brings about two folds of consequences on the above-barrier quasi-bound states: the one is the remarkable reduction of the level width of the quasi-bound states. Hence, it tends to result in the enhancement of optical absorption peak intensity; the other is the splitting of the above-barrier quasi-bound levels with different Landau quantum numbers, as shown in Figure 1 and in equation (21). Correspondingly, it leads to the splitting of the optical absorption peaks associated with these quasi-bound states. Hence, it is possible to detect the existence of the above-barrier magneto-quasi-bound states with different Landau quantum numbers in single barrier structures made of non-magnetic materials with use of the measurement of optical absorption spectrum.

3.4 Line-shape of resonant transmission peaks

As well known, the resonant tunneling peaks in the double-barrier structures have the well-defined Lorentzian line-shape when the level-width of the quasi-bound states is quite small, comparing with the absolute value of level and the level interval between two adjacent levels. As the physical mechanism of the above-barrier resonant transmission in single barrier structures is similar to that of

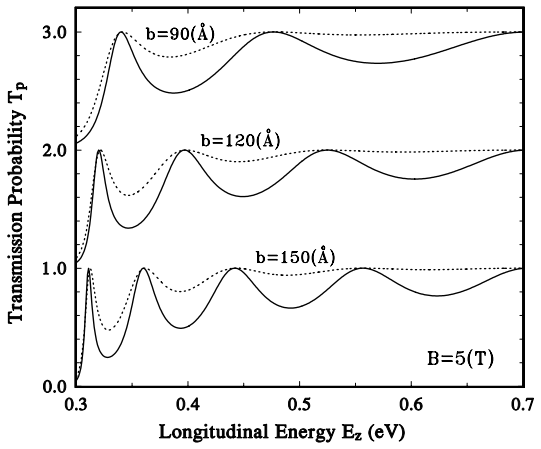

Fig. 3. Variation of the above-barrier transmission probability spectrum with the barrier width. Three sets of curves correspond to the barrier width of $b = 90$ Å, 120 Å, and 150 Å, from top to bottom. The consecutive sets of curves have been vertically shifted for clarity. The Landau quantum number is fixed at $N = 0$ and the magnetic field is $B = 5$ T. Dotted curves correspond to the case of neglecting the magnet-coupling effect, while solid curves to the case of including this effect.

the below-barrier resonant tunneling in the double-barrier structures, *i.e.*, both the resonant transmission and resonant tunneling are mediated by the quasibound states in these structures, so it is expected that the profile of individual resonant peak in $T_{\rm p}$ for single barrier structures may also have the well-defined Lorentzian line shape. However, at the first glance, the profile of individual peak in Figure 3 seems to be non-Lorentzian line-shape apparently. This is a false appearance. We guess that the superposition of the adjacent resonant peaks results in this false impression. When taking the overlap of the consecutive peaks into account, we may conjecture that the profile of the peaks in $T_{\rm p}$ spectrum can be described by the linear superposition of two Lorentzian functions. For instance, the line-shape of the first peak in Figure 3 can be expressed by

$$T_{\rm p}^1 = C_1 \frac{\Gamma_1^2}{(E_z - E_1')^2 + \Gamma_1^2} + C_2 \frac{\Gamma_2^2}{(E_z - E_2')^2 + \Gamma_2^2}, \quad (23)$$

where E_1' and E_2' are, respectively, the first and the second resonant levels, given by equations (21) and (22) with $m = 1$ or 2 for $B = 5$ T and $N = 0$. Γ_1 and Γ_2 are the half-widths of the corresponding resonant levels. According to the resonant conditions, *i.e.*, $T_{\rm p}^1 = 1$ at $E_z = E_1'$ and E_2', we can established two simultaneous equations for determining the coefficients of C_1 and C_2. Finally, C_1 and C_2 are given by

$$C_1 = \frac{(E_2' - E_1')^2 + \Gamma_1^2}{(E_2' - E_1')^2 + \Gamma_1^2 + \Gamma_2^2};$$
$$C_2 = \frac{(E_2' - E_1')^2 + \Gamma_2^2}{(E_2' - E_1')^2 + \Gamma_1^2 + \Gamma_2^2}. \quad (24)$$

Table 1. Half-widths of the first and second quasi-bound levels above the barrier. $\Gamma_i (i = 1, 2)$ correspond to the half-width of levels when neglecting the magneto-coupling effect and $\Gamma_i^{\rm mc}$ to that when including this effect for $B = 5$ T and $N = 0$.

b (Å)	Γ_1 (meV)	$\Gamma_1^{\rm mc}$ (meV)	Γ_2 (meV)	$\Gamma_2^{\rm mc}$ (meV)
90	30.4	18.4	135.0	65.2
120	12.6	7.8	53.2	29.0
150	6.3	4.0	25.6	15.2

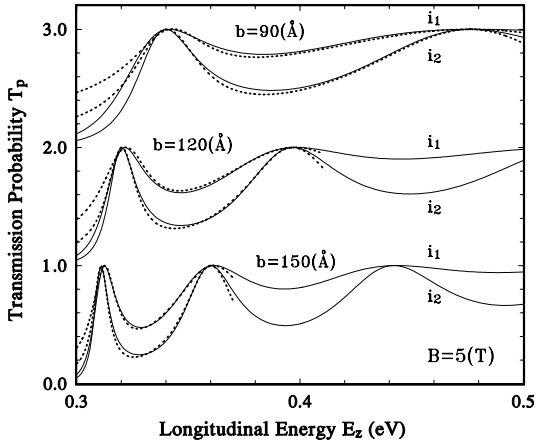

Fig. 4. Fitting results for the first resonant transmission peak in single barrier structures with different barrier widths as indicated in Figure 3. The relevant parameters are the same as in Figure 3. Dotted lines are the fitting results obtained with equation (23) in the text and solid lines are the exact results evaluated by equation (19) in the text. Curves labeled with i_1 correspond to the case of neglecting the magneto-coupling effect and curves denoted by i_2 to the case of including this effect.

To demonstrate the applicability of equation (23), we employ the method presented by Bahder *et al.* [17] to determine the half-widths of quasi-bound levels. The calculation results are listed in Table 1 [18]. It is clearly seen that the magneto-coupling effect results in the striking reduction of the half-width of the above-barrier quasi-bound levels. For example, the relative reductions of the line-width for the first quasi-bound level with $m = 1$ and $N = 0$ reach, respectively, to 39.5%, 38.1%, and 36.5% for $b = 90$, 120, and 150 (Å), at $B = 5$ T. We now substitute the parameters of Γ_i given in Table 1 and the values of E_1' and E_2' evaluated by equations (21) and (22) into the expression equation (23) of $T_{\rm p}^1$ to fit the accurate transmission probability curves. The fitting results are displayed in Figure 4. Dotted curves are the fitting results with use of the expression equation (23) and solid curves represent the accurate results given by equation (19). Curves labeled by i_1 correspond to the case of neglecting the magneto-coupling effect and curves labeled by i_2 to the case of including this effect. It is evident that the fitting curves are in good agreement with the accurate results. The smaller

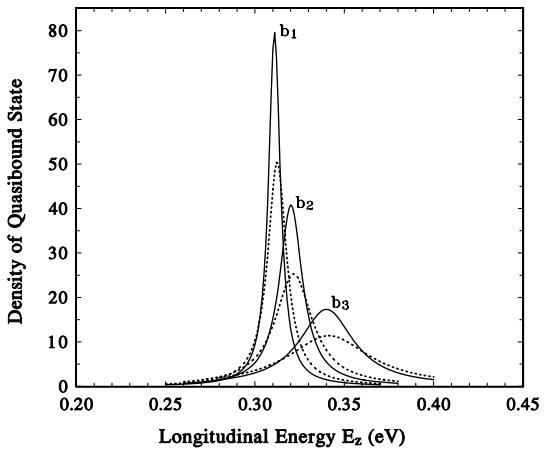

Fig. 5. Profile of density of the above-barrier quasi-bound states for single barrier structures with different barrier widths. Curves labeled by b_1, b_2, and b_3 show the densities of the quasi-bound states for barrier widths equal to 150 Å, 120 Å, and 90 Å, respectively. Dotted lines correspond to the case of neglecting the magneto-coupling effect and solid lines to the case of including this effect. The Landau quantum number is $N = 0$ and the magnetic-field intensity is $B = 5$ T.

the half-width of the quasi-bound levels is, the higher the fitting accuracy is. Therefore, our results clearly show that the individual resonant transmission peak in single barrier structures indeed has the well-defined Lorentzian line shape. So, we can deduce that the density of the above-barrier quasi-bound states in single barrier structures have Lorentzian form as follows [19]:

$$\rho_i(E_z) = \frac{\Gamma_i/\pi}{(E_z - E_i')^2 + \Gamma_i^2} \cdot \tag{25}$$

The numerical results for the lowest quasi-bound states are depicted in Figure 5 for three different barrier widths: curves marked by b_1 for $b = 90$ Å, by b_2 for $b = 120$ Å, and by b_3 for $b = 150$ Å. Dotted curves correspond to the case of neglecting the magneto-coupling, solid curves to the case of including this effect. As addressed above, the peak value of DOQBS rapidly increases as broadening the barrier width, and the magneto-coupling effect substantially enhances the value of DOQBS. Comparing Figure 5 in the present paper with Figure 3 in reference [11], it can be found that the profile of the DOQBS is quite similar to the line-shape of the peaks in optical absorption spectrum. It clearly demonstrates that the profile of the DOQBS in single barrier structures can be approximately described with high accuracy by equation (25). All of the above discussions on the line-shape of the above-barrier resonant transmission peaks and the density of the above-barrier quasi-bound states directly support the fact that the appearance of the above-barrier resonant transmission peaks is tightly related to the existence of the above-barrier quasi-bound states in single barrier structures.

4 Summary and remarks

In this paper, we have investigated the influence of the magneto-coupling on the transmission probability, tunneling time, and the above-barrier quasi-bound states in single quantum barriers in detail. Based upon the parabolic conduction-band approach, a modified one-dimensional effective-mass Schrödinger equation, including the magneto-coupling effect, is strictly derived to actually describe the longitudinal motion of electrons in semiconductor heterostructures. Numerical calculations for single barrier structures have shown that the magneto-coupling effect brings about a series of important consequences on the quantum features of the devices, such as the transmission probability $T_{\rm p}$, the tunneling time $T_{\rm t}$, and the above-barrier quasi-bound states.

We find that the magneto-coupling effect results in the remarkable enhancement of the below-barrier transmission probability $T_{\rm p}$ and brings about three folds of important changes on the above-barrier resonant transmission: the first is the appearance of the new, resolvable resonant transmission peaks; the second is the striking shift of the resonant peak positions associated with different Landau quantum numbers toward the low energy region; the third is the considerable reduction of the line-width of the resonant peaks. A very interesting resonance-like phenomenon is also found in the tunneling time $T_{\rm t}$ spectrum. The magneto-coupling effect always causes the increase of the tunneling time $T_{\rm t}$ and leads to the significant dependence of the resonance-like peak positions in $T_{\rm t}$ spectrum on both the magnetic-field intensity B and the Landau quantum number N.

Through examining the variation of the above-barrier $T_{\rm p}$ spectrum with the barrier width in single barrier structures, we find that the resonant peaks in $T_{\rm p}$ shift toward the low energy region and the line-widths of the resonant peaks rapidly narrow down as increasing the barrier width. With use of the half-width of the above-barrier quasi-bound levels and linear superposition of two Lorentzian functions, we can fit the line-shape of the first above-barrier resonant peaks very well. The smaller the half-width of the quasi-bound levels is, the higher the fitting accuracy is. All of the above results can be interpreted by the fact that the resonant transmission in single quantum barrier is generated from the multiple coherent reflections of the electronic wave function at two edges of single barrier scattering potential leading to quasibound states in the barrier region, and the magneto-coupling effect between the longitudinal motion and the transverse Landau orbits of an electron results in the enhancement of localization of the quasibound states. This is the reason why the line-width of the resonant peaks in $T_{\rm p}$ strikingly reduces and the transmission time $T_{\rm t}$ in the vicinity of the resonant levels remarkably increases when the magneto-coupling effect is taken into account.

According to the physical mechanism of the above-barrier resonant transmission in single quantum barriers, we come to the conclusion that the magneto-coupling effect leads to not only the splitting of the above-barrier quasi-bound levels associated with the different Landau

quantum numbers but also the reduction of the half-width of the quasi-bound levels, correspondingly, the substantial enhancement of density of the above-barrier quasi-bound states. Accordingly, the magneto-coupling effect results in the splitting of the optical absorption peaks and the striking enhancement of their intensities in single barrier structures. We suggest that the magneto-coupling effects may be observed with the measurements of the optical absorption spectrum in the single barrier structures.

The authors would like to thank the referee for his valuable comments and suggestions on revising and improving our manuscript. This work was supported by the National Natural Science Foundation of China.

References

1. U. Ekenberg, Phys. Rev. B **40**, 7714 (1989).
2. Timothy B. Boykin, R. E. Carnahan, R. J. Higgins, Phys. Rev. B **48**, 14232 (1993); Timothy B. Boykin, *ibid.* **51**, 4289 (1995).
3. D. J. Ben Daniel and C. B. Duke, Phys. Rev. **152**, 683 (1966). Phys. Rev. B **38**, 3994 (1988). Phys. Rev. B **38**, 3994 (1988).
4. G. Bastard, *Wave Mechanics Applied to Semiconductor Heterostructures* (Les Éditions de Physique, Les Ulis, 1990).
5. C.E.T. Gonqalves da Silva, E.E. Mendez,
6. X.H. Wang, B.Y. Gu, G.Z. Yang, Phys. Rev. B **55**, 9340 (1997).
7. V.V. Paranjape, Phys. Rev. B **52**, 10740 (1995).
8. X.H. Wang, B.Y. Gu, G.Z. Yang, Phys. Rev. B **56**, 9224 (1997).
9. X.H. Wang, B.Y. Gu, G.Z. Yang, Phys. Lett. A **234**, 233 (1997).
10. R. Beresford, L.F. Luo, W.I. Wang, E.E. Mendez, Appl. Phys. Lett. **55**, 1555 (1989).
11. H. Luo, N. Dai, F.C. Zhang, N. Samarth, M. Dobrowdska, J.K. Furdyna, C. Parks, A.K. Radams, Phys. Rev. Lett. **70**, 1307 (1993).
12. D.Y.K. Ko, J.C. Inkson, Semicond. Sci. Technol. **3**, 791 (1988).
13. Timothy B. Boykin, S. James, Jr. Harris, J. Appl. Phys. **72**, 988 (1992).
14. K.V. Rousseau, K.L. Wang, J.N. Schulman, Appl. Phys. Lett. **54**, 1341 (1989).
15. B. Lee, Superlatt. Microstruct. **14**, 295 (1993); B. Lee, W. Lee, *ibid.* **18**, 177 (1995).
16. R.Y. Chiao, P.G. Kwiat, A.M. Steinberg, Sci. Ame. **289**, 38 (1993).
17. T.B. Bahder, C.A. Morrison, J.D. Bruno, Appl. Phys. Lett. **51**, 1089 (1987).
18. $\Gamma_2 = 135.0$ meV in Table 1 is an optimal fitting value. It is large enough to make the method of reference [13] failure.
19. T. Wei, B. Vinter, Appl. Phys. Lett. **50**, 1281 (1987).